Development of WAAM process: slicer, robot trajectories, and examples of parts

Rodolphe BOLOT (rodolphe.bolot@u-bourgogne.fr)
Université de Bourgogne https://orcid.org/0000-0002-1481-7711
Alexandre MATHIEU
Maxime SIMON

Research Article

Keywords: WAAM, Wire Arc Additive Manufacturing, Metal Additive Manufacturing, slicer, automatic robot program generation, Offline Programming of robot trajectories

Posted Date: March 6th, 2023

DOI: https://doi.org/10.21203/rs.3.rs-2625492/v1

Abstract

This work is devoted to Wire Arc Additive Manufacturing processing. The question of automatic generation of robot trajectories is mainly addressed. An in-house slicer was first developed. Once the part to be manufactured has been designed and converted into STL format, the slicer allows automatic generation of successive vertices defining the part contours and corresponding robot trajectories. Automatic generation of the robot program is then performed including displacement instructions written in KRL language (case of KUKA robots), as well as commands related to the CMT welding device. The different steps in the offline programming pre-treatment process are first described. In a second step, two distinct parts with increasing degrees of complexity were printed using the corresponding offline programming tool. Finally, the question of the scanning strategy is discussed, the manufactured parts are shown, and required further improvements are explained.

1. Introduction

Wire Arc Additive Manufacturing has great potential to manufacture blanks of large metal parts. It benefits from various advantages such as the absence of a closed chamber under inert gas, or its very high deposition rate (up to about 3 kg/h). On the other hand, the resolution of manufactured parts is significantly lower than in SLM additive manufacturing for example (several mm wide cords, against typically 50 µm in SLM). It can therefore be used to produce quickly rough parts, that will then have to undergo finishing machining. It can also be used to make local adds of material to very large parts, thus simplifying the initial design of the part in question. At the present time, there are no fully integrated standard solutions provided by manufacturers, as is the case of SLM. And each one generally carries out their own homemade developments (laboratories and companies), in particular at the level of the software part. The objective of our work was to develop a complete tool meeting our specifications, and adapted to our available equipment (KUKA KR6 and KR60 robots, FRONIUS CMT workstation). Through this work, we present the specific developments made (CAD slicer, automation of trajectories generation, deposition strategy, examples of printed parts). Our objective was to quickly have a simple, easy-to-use and effective solution for the manufacture of blanks with potentially complex geometries.

Most studies devoted to WAAM concern characterization of material properties so that simple walls are often manufactured. Horgar et al. [1] have built Aluminum alloy parts (AA5183, i.e. Al4.5MgMn alloy) and produced tensile specimens oriented differently regarding to the aligned welds. In all cases, the ultimate tensile strength of their samples was a little below 300 MPa, with maximum strains in the range 22-29% depending on the sample orientation. Fuchs et al. [2] studied the machining allowance of Ti6Al4V near-net shaped WAAM parts in the frame of aeronautic industry. Rodrigues et al. [3] compared conventional GMAW WAAM and UC-WAAM in which the electric arc is established between the wire feedstock material and a non-consumable tungsten electrode. According to the authors, a potential advantage of UC-WAAM was that the layers can be deposited on a non-conductive material, which can allow producing overhang structures without any support: this advantage can be useful to manufacture complex structures. If one looks for the combination of WAAM and robot in the title of articles in the literature, only two articles are

listed: Gurcik and Kovanda [4] used a FANUC robot with off-line programming to generate their trajectories. They illustrated the problematic of trajectory defaults, as well as that of defects caused by the variation of the wire feeding speed. However, they finally manufactured quite simple parts (cylinders with a height of almost 60 mm) that could have been efficiently produced with a few lines of robot commands defining a circle by just three vertices, and including a repeating loop. The second one is by Schmitz et al. [5] and deals with multidirectional WAAM additive Manufacturing (i.e., the possibility to build up layers in all directions). In this work, the question of path planning in WAAM is discussed, as well as interfacing with the CAD of the part to manufacture. In particular, the intersection between triangular faces described in a STL file with a horizontal plane results in a polygonal cross-section of the component along this plane. Depending on the part complexity, the result may either be a single polygonal line of multiple polygons separated each other or imbricated one in the other (case of a hollow part). For a multidirectional slicing strategy, some parts of the geometry may be sliced in one direction, whereas some other parts are scanned in a different direction. Among works cited by Schmitz et al., one can mention that of Ding et al. [6] about slicing of STL models for WAAM purpose. In particular, they showed the structure of ASCII STL files created by software products such as CREO or FREECAD. In their work, they subdivided the geometry into multiple volumes in order to allow applying different slicing directions depending on the considered subpart. In another article [7], Schmitz et al. used their method to print a simple elliptical half-shell. Concerning welding, Fang et al. [8] used CAD data to define the path of the weld in the case of Y-type intersection of ducts. Venturini et al. [9] discussed the strategy for manufacturing of T-crossing features. Knezovic et al. showed several parts concerned with this strategy [10]. However one can notice that the geometrical complexity is moderate for this type of part, since all deposited layers show the same shape, so that a loop can be used with a progressive upgrade of the Z coordinate. The strategy consists in selecting the most adapted sequence of alternating path. Ali et al. [11] studied the effect of different paths to manufacture a flat part from juxtaposed welds. They showed that the resulting Von Mises stress and displacement fields is different depending on the selected scanning trajectories. Reisgen et al. [12] tested different cooling methods and showed their influence on the $t_{8/5}$ time (i.e., the time it takes for the weld seam to cool from 800°C to 500°C). The results were then correlated to the Vickers hardness. Finally, Rodrigues et al. [13] proposed an article showing the current status and perspectives of WAAM in terms of processes (variants and declinations), in-situ cooling and substrate preheating strategies, material types, deposition strategy, residual stresses, post heat-treatments, and of course applications.

The aim of the present study is to show our recent developments performed in the frame of the COBAFIL project, financed by the Bourgogne Franche-Comté Region (France). This project is mainly focused on the development of a vision based online system for the control of the wire arc additive manufacturing process. The final objective is to compensate the effect of defects such as variation of the thickness of individual welds during the manufacturing process of parts. As preliminary part of the work, an in-house offline programming (OLP) software was developed in order to generate automatically the command files of the robot/welder system from the CAD file of the part to build. Up to now, the case of shell type parts

was considered, since it presents several applications especially in the objective of parts weight reduction. The objective of the present work is thus to show the different steps of the OLP software (i.e., STL file, slicer, trajectories, and robot/welding device command files). The present solution is certainly very similar in comparison with that developed by Schmitz two years ago [5,7]. The first step concerns the choice of a CAD package to import or draw the part to be printed by WAAM. In our work, it was decided to work with free software products only, so that FreeCAD was selected. FreeCAD [14] is a free and open source CAD software. It allows using solid modeling, functional modeling, as well as surface modeling. In addition, it allows exporting the designed parts in STL ASCII format, which is quite easy to read with any programming language, such as C.

Figure 1 shows the typical structure of an ASCII STL file. All triangular faces are defined individually from the Cartesian coordinates of three vertices. It is thus easy to read such file and to define the three edges connecting the vertices. In principle, only one other face is connected to each edge (i.e., only two faces share a common edge). It is also easy to calculate the coordinates of the two vertices defining the intersection with a horizontal plane (if it exists). Finally, intersection of a horizontal plane with a solid defined in a STL file, consists in connected edges forming at least one closed polygon (possibly several ones).

It is thus possible to define the different polygons corresponding to the intersection of solids defined in the STL file, with a series of slices (for example series of Z altitude). Finally, it is the role of the slicer to do this work, and to provide the different polygons through a series of successive vertices. In a second step, it is possible to convert the series of vertices in a series of KRL instructions [15] defining the robot trajectory (case of a KUKA robot). In addition, it is possible to add instructions for arc ignition (start of a polygon) and arc extinction (end of a polygon). The connection between two successive polygons may be defined by an additional straight line, and the corresponding displacement instruction may be added: during this connection, the arc of the welder is off. Figure 2 shows a concrete example for the case of a simple part composed of a brick, a cylinder, and a conical part. The STL mesh generated by FREECAD is shown at the left, and the corresponding slices are shown at the right (plot of the successive lines with SCILAB [16], including connections between successive slices). Even if all slice contours look like circles in the top part, these circles are formed by straight edges, forming closed polygons. In the present case, the different slices are formed by a little more than 2200 straight edges.

2 Manufacturing Of Simple Walls And Adjustment Of The Deposition Strategy

Preliminary experiments based on printing of simple beams were performed prior printing more complex parts with the OLP tool. These experiments were conducted in order to:

- define a set of suitable welding parameters

- correct defaults before printing real parts and select a scanning strategy

For these experiments, a FRONIUS CMT welding apparatus was used.

Figure 3 shows the result of our very first beam printed by WAAM. This beam was printed before the development of our OLP tool and was made of 15 different layers, starting from the left, and ending at the right for each weld bead. One may easily note that the height of the beam shows a decreasing trend from the left to the right. In particular, it is significantly higher at the left side, where the arc was ignited for each layer. From this result, we decided to alternate the scanning direction for printing of each layer, for the next experiments. In addition, it was also decided to avoid igniting the arc at the same place for each layer. Thus, in the OLP tool we developed:

- the scanning direction is alternated for each successive layer
- the starting point (where the arc is ignited) is positioned at the opposite side of the polygon each 2 layers

It is the reason why one may notice de presence of almost horizontal lines connecting the ending point of a layer to the starting point of the next one (Fig. 2 right).

3. Structure Of A Krl File Automatically Generated For A Kuka Robot

Figure 4 shows the typical structure of a KRL src file automatically generated by our OLP tool. The part that is shown is just between two successive polygons. First, each displacement between successive points of a polygon is achieved with a LIN command allowing displacing the TCP point linearly from the current position to the specified point. In the example POSREF represents a reference position corresponding to that of the origin of the part to manufacture in the CAD model. In addition, the C_DIS option of LIN commands allows avoiding stops on each intermediate point (with subsequent slowdown), and continuing displacing with the specified speed. When the contour of a polygon is finished, the arc is switched off and the welder displacement is stopped on the last point during a time laps of a few seconds (during which the gas of the welding device contributes to cool the part). Then, the welder moves linearly from the current position to the first point of the next polygon, the arc is then ignited again and the welder moves linearly to successive points of the next polygon. In next version of the program, all LIN commands with C_DIS option could be replaced by SPL commands, allowing defining SPLINE curves. However, SPL commands are not implemented in the former version of our robot command system: an upgrade will be operated during February 2023. Anyway, it is not clear whether or not the deposition process will be improved using SPL commands, since LIN commands with C_DIS option provides satisfactory results. Finally, suppression of short edges along polygons is not required but may just allow decreasing the number of points and the size of files. One may remark that the three angles defining the tool orientation at each point are kept unchanged, meaning that the welding device remains vertically aligned: this choice allows avoiding strong accelerations where the skeleton of the part shows direction

changes. However, it is envisaged to follow the wall orientation for some type of parts, and especially for parts presenting smooth variations of the curvature without abrupt direction changes.

4. Manufacturing Of Reals Parts And Discussions

Once the OLP tool was finalized and tested, it was then possible to use it to print complex parts. The retained deposition parameters are listed in Table 1.

Table 1: Deposition parameters

Material (wire)	316 L stainless steel
Wire diameter (mm)	0.8
Wire feed rate (m/min)	12.5
Current intensity (A)	128
Current voltage (V)	16
Welding gas	Ar
Welding mode	CMT
Welding speed (m/s)(m/min)	0.0125-0.75

Using these parameters and neglecting material losses, the expected value of the cross-section of individual weld beads may be estimated from:

$$S_{weld} = S_{wire}\frac{V_{wire}}{V_{weld}} = \frac{\pi 0.8^2}{4}\frac{12.5}{0.75} = 8.4\ mm^2$$

Considering an average wall width of 6 mm, the expected height of each weld bead is thus 1.4 mm.

In the real life, experiments performed with this set of parameters showed that the average height of each deposited bead was about 1.5 mm. This value is not so different and the weak variation is certainly related to a small overestimation of the average thickness of the wall, which has dips and bumps. Anyway, a decrease of the height of the weld bead was noticed for short waiting time between successive layers (i.e., for a high sublayer temperature), whereas the height of 1.5 mm was confirmed when increasing the waiting time between layers (typically up to 10 seconds or more).

The case of more complex parts was thus considered with this set of welding parameters. The objective was to show the feasibility of the automated manufacturing process. Printing of two different shell type parts is reported in the next section.

Figure 5 illustrates the first one consisting in a part with regular pentagon basis (5x 50 mm edges at the bottom, 5x108° between successive 5 edges). The total height of the part is 97 mm: bottom part 21 mm +2x38 mm in the upper part. In addition, the dimension of the 5 edges at the largest section is 63.5 mm. The right picture shows the simplest STL file that can be generated in the present case: each quadrangle is split in two triangles, whereas the bottom and top pentagons are split with 3 triangles, resulting in a total number of 36 triangular faces (i.e., 15x2 +2x3). Slicing of this part with horizontal planes results in a series of polygons composed 10 edges (1 intermediate vertex along each straight edge of the pentagon).

Direct in-situ coding of the robot program required to print this part would be quite complex. On the contrary, the OLP tool allows generating the corresponding list of instructions in less than one second, once the SLT file is produced. With the OLP tool there are only few parameters to adjust, such as the name of the STL file to consider and the number of slices (or height between successive slices). In addition, the generated list of instructions is always free of bugs once the program has been tested and validated. Once back on the real robot cell, only the POSREF position must to be defined by learning. It corresponds to the position at which the part will be printed.

Figure 6 shows the corresponding robot trajectories viewed with SCILAB software including lines connecting successive slices (start at the opposite side for two successive slices). The starting point of each slice is always one of the vertices along the trajectory (i.e., one of the 10 points defining each pentagon for the present part). In the present case, it may either be one of the pentagon corners or the single intermediate point on each straight edge of the pentagon. These points are thus often aligned or regularly staggered. In order to avoid that, a simple strategy can consist in increasing the number of triangles in the STL file, for example by forcing a maximum edge length of 10 or 20 mm for triangles. By doing so, the starting point of each slice (where the arc ignition takes place) would be more randomly distributed.

Figure 7 shows the corresponding part at different steps during WAAM printing. The part was manufactured by applying the aforementioned strategy: starting point of a polygon at the opposite side regarding the previous one + inversion of the rotation direction for each layer. This strategy allows avoiding amplifying the thickness differences, such as that observed on Fig. 3. In details, the weld gun turned clockwise for images 1 and 3 (left), and in the counterclockwise direction for images 2 and 4 (right).

Figure 8 shows the corresponding part after complete cooling and slight hand brushing of the surface (left) and after machining of external surfaces (right). No significant distortion was observed during machining of flat surfaces, and during machining of the word PFT3D (one letter per face). However, the residual thickness of the metal sheet is thin in places: the question of optimum positioning of the final part in the blank is thus a concern. Finally, simple experiments showed that the final part is weakly magnetic, which confirms that it is not composed of austenitic g-phase only. The d-ferrite phase can form at high temperature and probably appeared during the manufacturing process. This phase may allow decreasing the risk of hot cracking if its content is lower than 8%. However, it can be detrimental to the

corrosion resistance if its content becomes higher than 10%. According to the Schaeffler diagram, the ferrite content of 316L steel after solidification and cooling should be about 5%, which is probably the case of 316L steel manufactured by WAAM.

The second part example is shown in Figure 9: it consists in a double square to circular transition part (i.e., square to circular transition, followed by a circular to square transition). The dimensions of the bottom and top square sections are 80x80 mm, whereas the diameter of the circular part at mid height is 60 mm. The total height of the part is 150 mm. This part is thus much more complex, including nonplanar curved surfaces. The corresponding STL file is composed of 1940 triangular faces, but the OLP program remains efficient as well.

Figure 10 shows the resulting robot trajectories including connecting edges between successive slices, used to alternate the position of the starting point for each weld bead. The resulting number of vertices, edges and displacement instructions in the robot file is as high as 7155 for this example.

Figure 11 shows the printed part after brushing. It has no major flaws and is ready for machining of functional surfaces. In the best case, only the inner diameter of the circular part, and flat faces of the square sections could be relevant for machining, whereas some other faces could be let as raw. If all surfaces have to be machined, the existing CAD design of the part could also be used to perform the corresponding machining using a CNC machining center. Potential applications of the technology are numerous. One of them concerns the rapid fabrication of complex shape powder containers for the Hot Isostatic Pressing technology. In particular, a HIP press was recently purchased in the frame of Equipex+ CALHIPSO, and will soon be available on the technology site of Le Creusot. The WAAM technology including robot offline programming from the CAD of the part could thus be particularly useful in this frame.

Up to now, the main remaining challenge to meet concerns the accuracy of the thickness of each layer, regarding to initial expectations. For the first case exposed, the total height of the first printed part was slightly lower in comparison with that which was initially expected (i.e., about 95 mm instead of 97 mm in the CAD model). A lengthening of the waiting time allowed us to correct this small mismatch in a second step (i.e., second printing of the same part). However, it would be preferable to avoid iterative printing. One idea to meet the challenge could consist in online control of the deposited thickness of each layer, or at least online control of the part height during the deposition process. In that case, one may imagine to modify somewhat the structure of the program, in order to allow repeating several times a layer if required (i.e., if the part height after a given layer is lower than the theoretical expected one). Another subsequent default correlated to the same reason is the progressive increase of the stick-out (i.e., distance between the welding gun and the part) if the deposited thickness becomes lower than that expected: this drawback would also be offset by an online control of the thickness or of the part height. However, it was checked that the thickness of the deposited weld bead is dependent on the sublayer material temperature (i.e., the bead thickness decreases somewhat if the sublayer temperature is too high). The first step before any control of the part height is thus in-situ control of the part temperature: the idea could thus be

to adjust automatically the waiting time between successive weld beads in order keep the part temperature unchanged during the whole manufacturing process. The required structure changes in the robot program is already defined, and the last step to reach our objectives concerns data exchange between the measurement system and the robot program. Finally, it is the subject of the COBAFIL program financed by the region of Bourgogne Franche-Comté, which aims at developing an online control system based on sensors and vision means.

5. Conclusions

The aim of the present study was to illustrate the capacities of our in-house OLP (Offline Programming) tool, allowing providing directly the list of instructions of the robot program required to manufacture a part by WAAM, from the CAD file of the corresponding part in STL format. The functionalities of this tool are certainly very similar to those of the tool developed by Schmitz 2 years ago. Nevertheless, additional information, advices and examples were provided. This tool produces very clean files and applies always the same method, which reinforces the robustness and interest of the method. The case of a deposition process managed by a KUKA robot was considered, so that the OLP tool provides the suitable list of instructions in KRL format. Of course, all robot manufacturers have their own input language. However, they often all have the same functionalities, so that it is highly probable to find corresponding instructions for each robot manufacturer. It is thus highly probable that our tool could be used to generate programs for several manufacturers, including only small changes (i.e., probably only the export function would have to be changed). This tool is thus certainly easily transposable to different types of robots. The question of filling the part may also be of interest: for this, the required function(s) will be written in a close future. However, manufacturing of shell type parts has already several applications especially in the frame of weight reduction. Finally, the present automated WAAM process is particularly adapted to manufacture blank parts.

Declarations

Fundings

This work was supported by the EIPHI Graduate School (Grant number ANR 17-EURE-0002) and Bourgogne-Franche-Comté Region.

Competing Interests

The authors have no relevant financial or non-financial interests to disclose

Author Contributions

Rodolphe BOLOT and Alexandre MATHIEU contributed equally to the development of the automatic robot trajectories generation tool, to the manufacturing of parts, and to the redaction of the article

Maxime SIMON contributed to the finishing machining of parts

References

1. A. Horgar, H. Fostervoll, B. Nyhus, X. Ren, M. Eriksson, and O.M. Akselsen, Additive manufacturing using WAAM with AA5183 wire, Journal of Materials Processing Technology, Volume 259, 2018, Pages 68-74.
2. C. Fuchs, D. Baier, T. Semm, and M.F. Zaeh, Determining the machining allowance for WAAM parts, Production Engineering, 14, 2020, Pages 629–637.
3. T.A. Rodrigues, V.R. Duarte, R.M. Miranda, T.G. Santos, and J.P. Oliveira, Ultracold-Wire and arc additive manufacturing (UC-WAAM), Journal of Materials Processing Technology, Volume 296, 2021, 117196.
4. T. Gurčík, and K. Kovanda, WAAM Technology optimized by off-line 3D Robot Simulation, 2019, Acta Polytechnica, Volume 59 (4), 2019, Pages 312-321.
5. M. Schmitz, J. Wiartalla, M. Gelfgren, S. Mann, B. Corves, and M. Hüsing, A Robot-Centered Path-Planning Algorithm for Multidirectional Additive Manufacturing for WAAM Processes and Pure Object Manipulation, Applied Science, 2021, 11, 5759.
6. D. Ding, Z. Pan, D. Cuiuri, H. Li, N. Larkin, and S. van Duin, Multi-direction slicing of STL models for robotic wire-feed additive manufacturing. In Solid Freeform Fabrication Symposium; The University of Texas at Austin: Austin, TX, USA, 2015, Pages 1059–1069.
7. M. Schmitz, C. Weidemann, B. Corves, and M. Hüsing, Trajectory Planning Strategy for Multidirectional Wire-Arc Additive Manufacturing. In ROMANSY 23—Robot Design, Dynamics and Control; Springer: Berlin/Heidelberg, Germany, 2020, Pages 467–475.
8. H.C. Fang, S.K. Ong, A.Y.C. Nee, Robot path planning optimization for welding complex joints, Int. J. Adv. Manuf. Technol., Volume 90 (2017), Pages 3829–3839.
9. G. Venturini, F. Montevecchi, A. Scippa, and G. Campatelli, Optimization of WAAM Deposition Patterns for T-crossing Features, Procedia CIRP, Volume 55, 2016, Pages 95-100.
10. N. Knezovic, and A. Topic, Wire and Arc Additive Manufacturing (WAAM) - A New Advance in Manufacturing, NEW TECHNOLOGIES, DEVELOPMENT AND APPLICATION, Volume 42, 2019, Page 65-71.
11. M.H. Ali, and Y.S. Han, Effect of Phase Transformations on Scanning Strategy in WAAM Fabrication, Materials, 14, 2021, 7871.
12. U. Reisgen, R. Sharma, S. Mann, and L. Oster, Increasing the manufacturing efficiency of WAAM by advanced cooling strategies, WELDING IN THE WORLD, Volume 64, 8, 2020, Pages 1409-1416.
13. T.A. Rodrigues, V. Duarte, R. M. Miranda, T.G. Santos, and J. P. Oliveira, Current Status and Perspectives on Wire and Arc Additive Manufacturing (WAAM), Materials, 12, 2019, 1121.
14. https://www.freecadweb.org/ (link accessed and valid in date of june 3, 2022)
15. http://robot.zaab.org/wp-content/uploads/2014/04/KRL-Reference-Guide-v4_1.pdf

16. **https://www.scilab.org/ (link accessed and valid in date of june 3, 2022)**

Figures

```
facet normal 0.000000 0.000000 -1.000000
  outer loop
    vertex 25.520000 -0.000000 -0.000000
    vertex -20.645252 15.000000 -0.000000
    vertex 7.886443 24.270510 0.000000
  endloop
endfacet
facet normal -0.000000 -0.000000 -1.000000
  outer loop
    vertex -20.645252 -15.000000 0.000000
    vertex -20.645252 15.000000 -0.000000
    vertex 25.520000 -0.000000 -0.000000
  endloop
endfacet
```

Figure 1

Typical structure of an ASCII STL file.

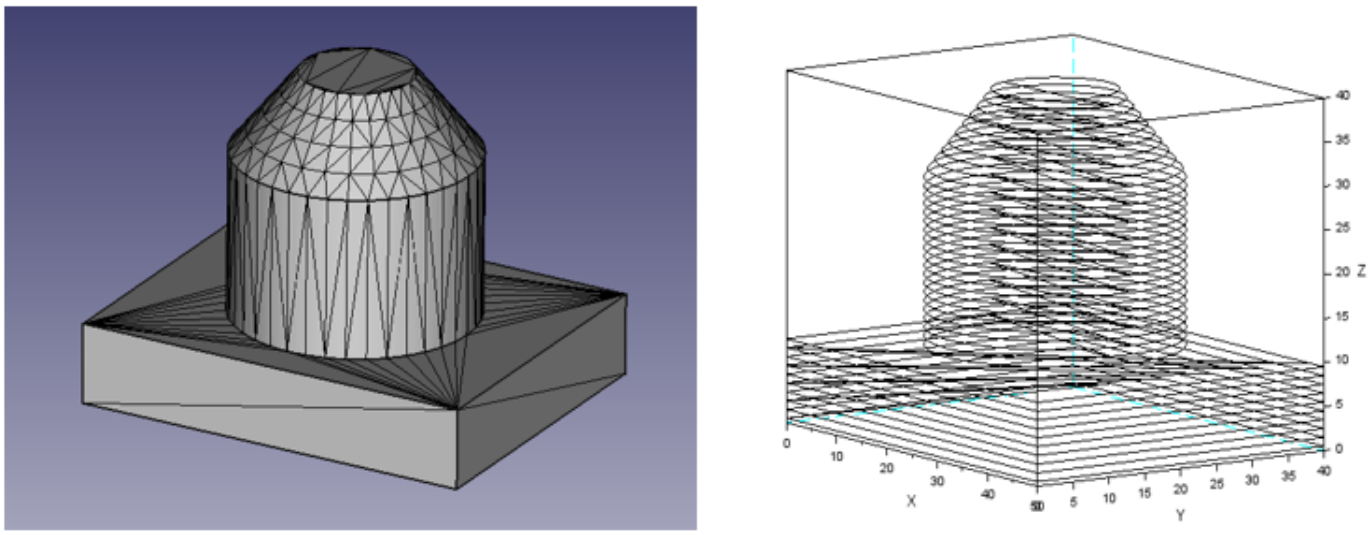

Figure 2

Simple CAD part viewed in FreeCAD (left) and corresponding slices viewed with SCILAB (right).

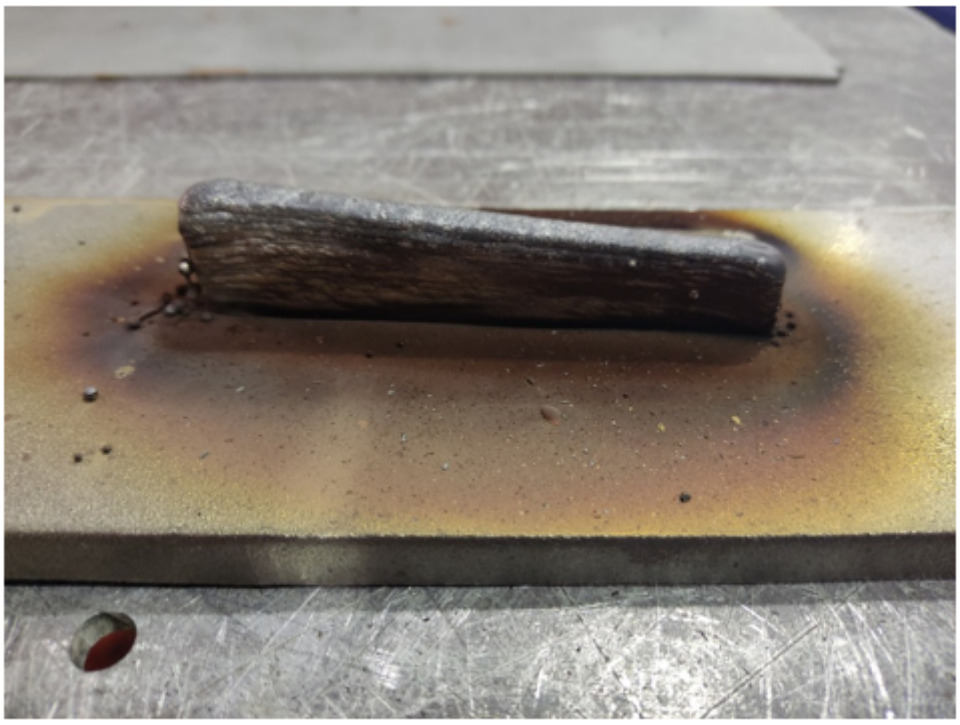

Figure 3

Beam printed during our first WAAM experiment (15 layers, all welds manufactured from the left to the right).

```
LIN POSREF:{X -10.247248,Y -35.087479,Z 5.319844, A 90.0,B 0.0,C 135.0} C_DIS
LIN POSREF:{X -40.450851,Y -13.143278,Z 5.319844, A 90.0,B 0.0,C 135.0} C_DIS
LIN POSREF:{X -36.536751,Y -1.096916,Z 5.319844, A 90.0,B 0.0,C 135.0} C_DIS
LIN POSREF:{X -25.000000,Y 34.409550,Z 5.319844, A 90.0,B 0.0,C 135.0} C_DIS
PRE_ARC_OFF_MSD(AMDWW1)
ARC_OFF_MSD()
WAIT SEC TPOSTGAS
;ENDFOLD SPLINE S3

; FOLD SPLINE S4
$BWDSTART = FALSE
LDAT_ACT=LCPDAT1
FDAT_ACT=FP1
BAS(#CP_PARAMS,VSOUD)
LIN POSREF:{X 40.450851,Y -13.143278,Z 6.835469, A 90.0,B 0.0,C 135.0}
PRE_ARC_ON_MSD(AMDSS,#UNSYNC_ARC)
ARC_ON_MSD(AMDSS)
WAIT SEC TWAIT1
LIN POSREF:{X 30.029228,Y 18.931175,Z 6.835469, A 90.0,B 0.0,C 135.0} C_DIS
LIN POSREF:{X 25.000000,Y 34.409550,Z 6.835469, A 90.0,B 0.0,C 135.0} C_DIS
LIN POSREF:{X -8.725075,Y 34.409550,Z 6.835469, A 90.0,B 0.0,C 135.0} C_DIS
LIN POSREF:{X -25.000000,Y 34.409550,Z 6.835469, A 90.0,B 0.0,C 135.0} C_DIS
```

Figure 4

Typical structure of a KRL src file automatically generated from successive slices (i.e. polygons such as those shown in Fig. 2)

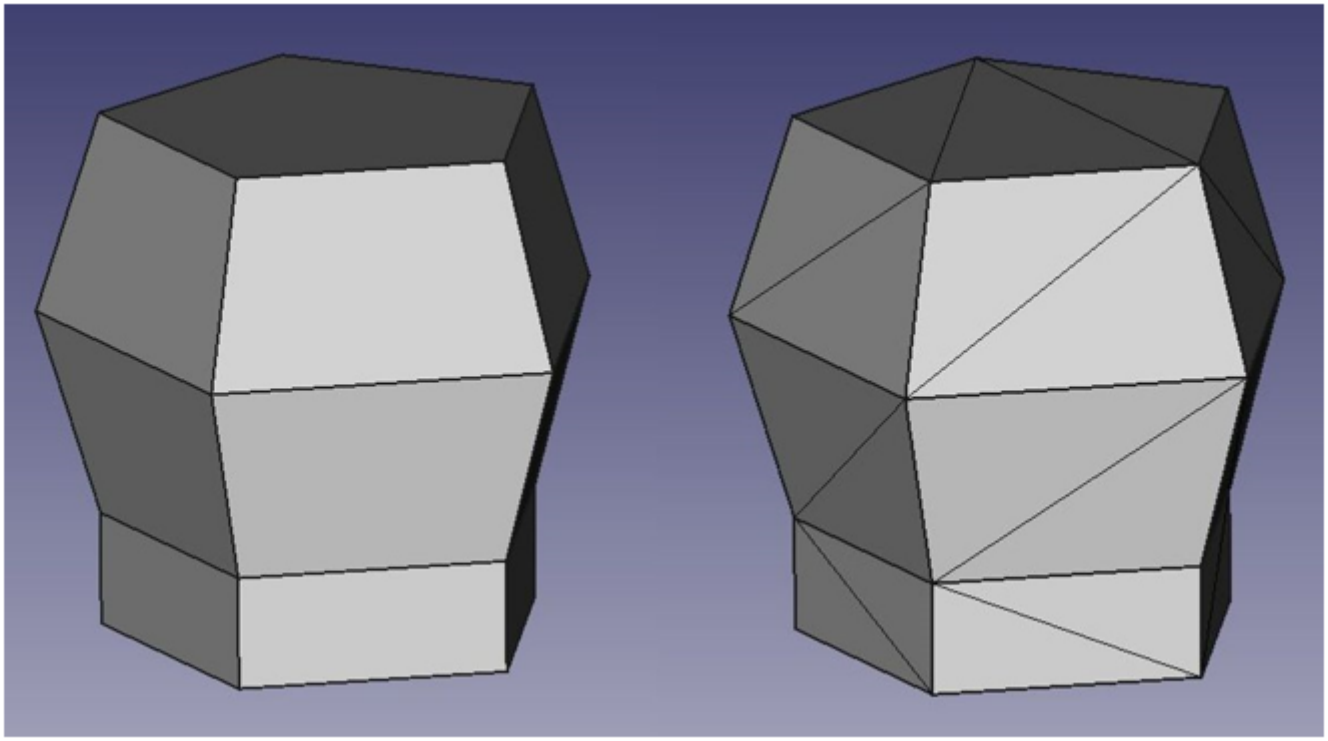

Figure 5

CAD view of the first part composed of a regular pentagon as basis (part height 97 mm, bottom edges 5x50 mm)

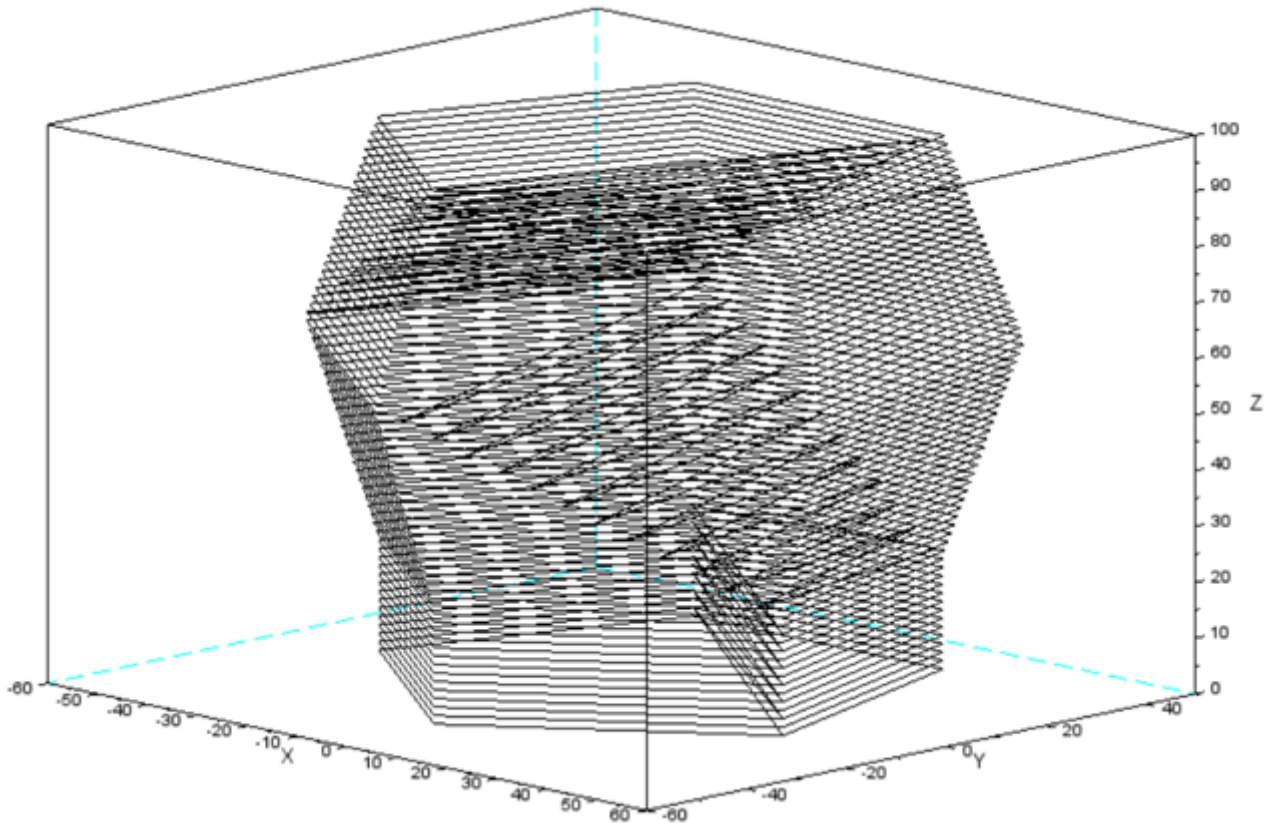

Figure 6

View of robot trajectories provided from the slicer and scanning strategy (inversion of the rotating direction at each slice and change of the starting point of successive slices)

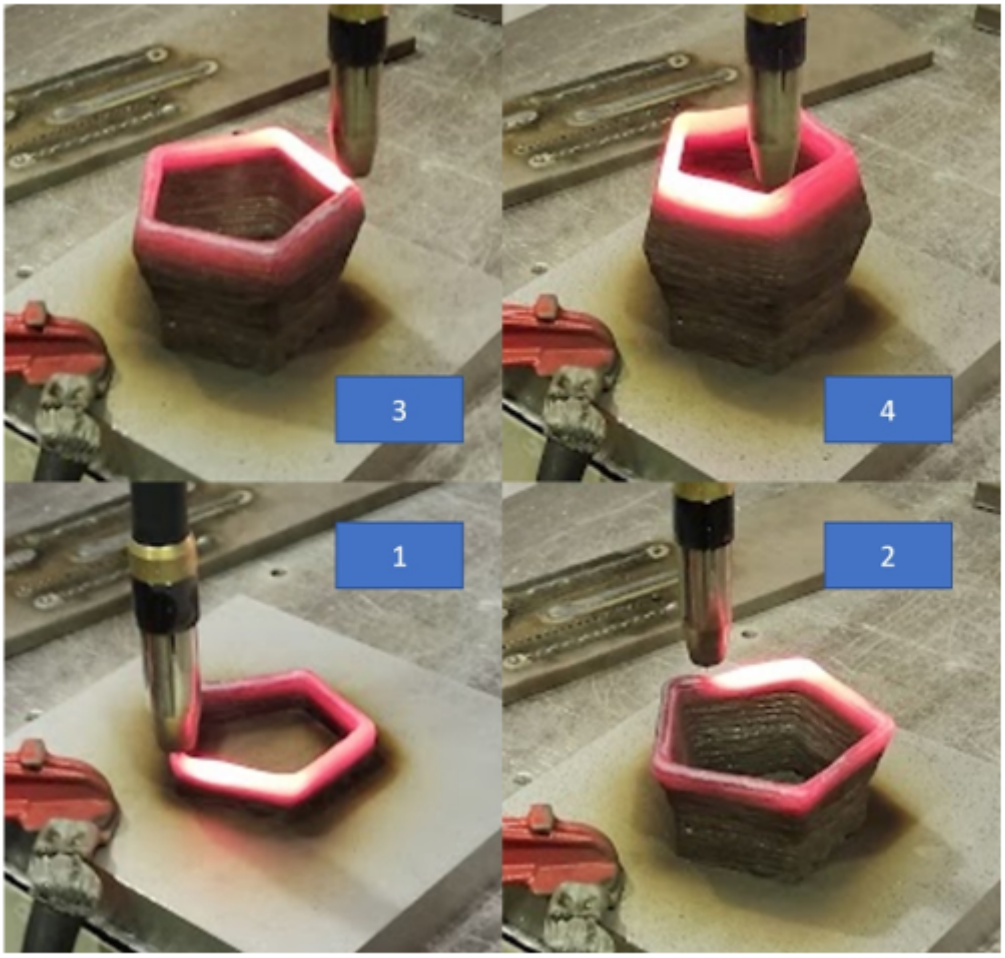

Figure 7

View of the part at four different steps during the manufacturing process.

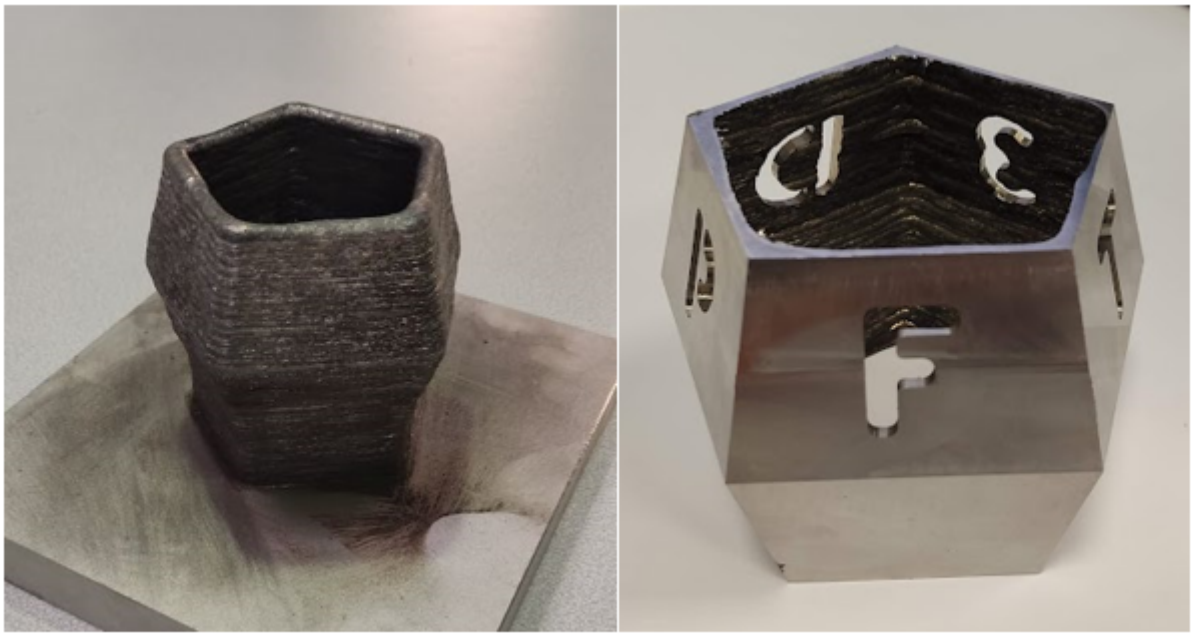

Figure 8

Corresponding part printed by WAAM process, before machining (left) and after machining of external surfaces (right).

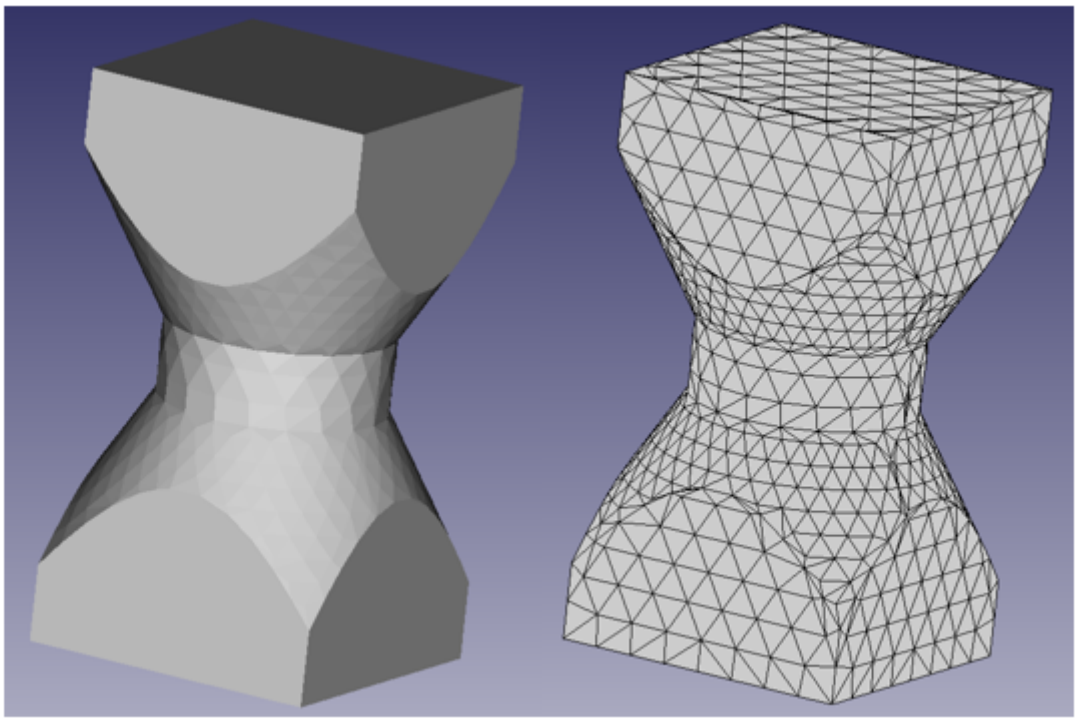

Figure 9

Views of the STL file of a part with successive transitions from square to circular, and square again, thus including nonplanar curved surfaces.

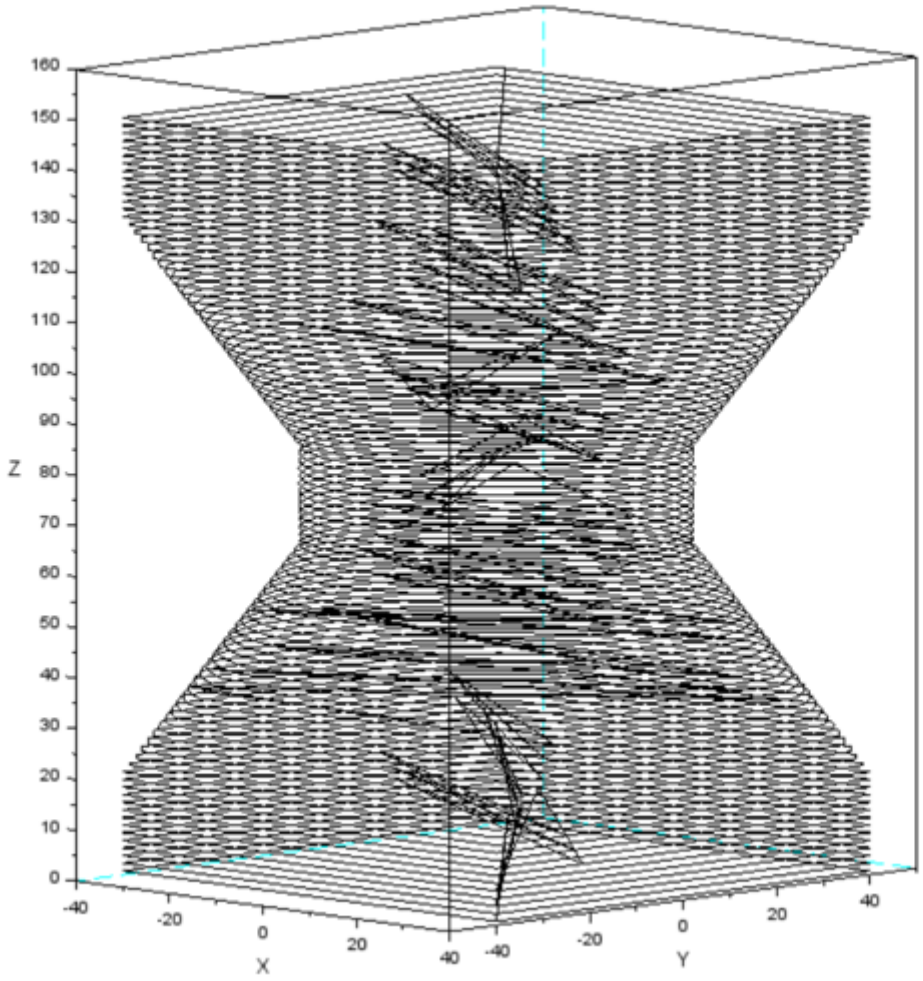

Figure 10

Resulting robot trajectories generated with the automatic slicer.

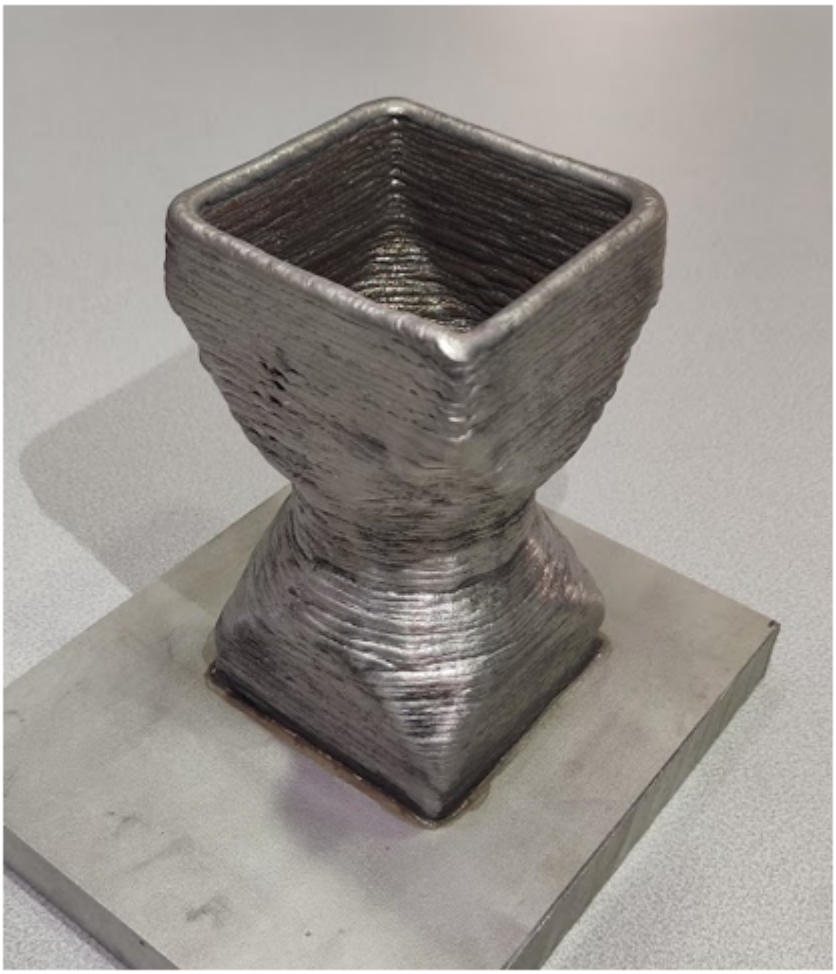

Figure 11

View of the printed part corresponding to the part shown on Fig. 9, and robot trajectories shown on Fig. 10.